Electron Microscope Image Contrast for Thin Crystals

J. M. COWLEY and SUMIO IIJIMA *

Department of Physics, Arizona State University, Tempe, Arizona 85281

(Z. Naturforsch. **27 a**, 445—451 [1972]; received 23 November 1971)

Dedicated to Prof. Dr. K. MOLIÈRE *on the occasion of his sixtieth birthday*

High resolution electron microscope images showing the detailed distribution of metal atoms within the unit cells of complex oxide structures have been recorded recently and as a first approximation may be interpreted as amplitude-object images if obtained with the degree of defocus corresponding to the "optimum-defocus condition" for the phase-contrast imaging of thin phase objects. Detailed observations of images of $Ti_2Nb_{10}O_{29}$ crystals having thicknesses of the order of 100 Å reveal that the thin phase-object approximation, which assumes that only small phase-shifts are involved, is inadequate to explain some features of the image intensities including the variation of contrast with crystal thickness. A very aproximate treatment of the phase contrast due to defocussing of phase objects having large phase shifts is evolved and shown to give a qualitativity correct account of the observations. The variation of image contrast with tilt away from a principle orientation is discussed. From the symmetry of the image contrast it is deduced that the symmetry of the crystal structure as derived from X-ray diffraction studies can not be correct.

1. Introduction

While the resolution of fringes having periodicities corresponding to crystal lattice plane spacings has been used for a number of years as a test for the instrumental stabilities of electron microscopes, the use of lattice imaging as a means of deriving useful information concerning crystal structures and their defects is relatively recent. It is well-known that the scattering of electrons by crystals is strongly dependent on the crystal orientation. Except in very favorable cases, it is therefore necessary to define the orientation of the crystal with precision by use of a goniometer stage if the images of crystals are to be interpreted in detail. Until recently the use of a goniometer stage has limited the resolution attainable to perhaps 10 or 15 Å which is not sufficient to give useful information on crystal structures except for major features of structures having large periodicities.

It has been shown by ALLPRESS and collaborators[1,2,3] that with a resolution of about 6 Å it is possible to derive a great deal of useful information regarding the structures of some complex oxide phases and the nature of the defects associated with their non-stoichiometry. While much of this information could be deduced from an observation of periodicities only, with the aid of some preknowledge gained by X-ray diffraction of the type of structures to be expected, these authors showed that it is possible to associate particular features of the contrast with particular groupings of atoms. Regions containing a higher concentration of metal atoms could be imaged consistently as dark spots.

Using an instrument with better resolution, UYEDA et al.[4] have obtained images of crystals of a phthalocyanine derivative in which the outline of the molecule can be traced. These authors made use of the "optimum defocus condition" proposed originally by SCHERZER[5] and applied by others[6,7,8] as a means for obtaining amplitude contrast from thin specimens of biological material which can be described as thin phase objects. For crystals having a thickness of the order of 100 Å and containing relatively heavy atoms it would seem unlikely that this simple theory, which assumes that only small phase-changes occur, should be applicable. However the observations by IIJIMA[9] on images having a resolution of about 3 Å, obtained from some complicated titanium-niobium oxide structures, suggest that an interpretation in terms of this theory may be possible. Images taken with the prescribed underfocus of about 900 Å show a darkening dependent on the number of metal atoms present in the projection of the crystal structure in the direction of the incident beam. For example, in Fig. 1 (a) and (b)** the image of a crystal of $Ti_2Nb_{10}O_{29}$ is compared with a diagram

Reprint requests to Prof. Dr. J. M. Cowley, Department of Physics, Arizona State University, *Tempe, Arizona* 85281, *U.S.A.*

* On leave from Research Institute for Scientific Measurements, Tohoku University, Sendai, Japan.

** Figures 1, 3, 6 and 7 on p. 448 a, b.

of the structure as deduced from the X-ray diffraction study by WADSLEY[10]. The image was obtained with the incident beam in the direction of the short b-axis of the unit cell, giving the diffraction pattern of Fig. 1(c) in which a circle has been drawn to indicate the size of the objective aperture and so the portion of the diffraction pattern which contributes to the image. Positions in the unit cell where there is one isolated metal atom per unit cell in the projection of the structure appear grey. Positions where two metal atoms are close together in the projection appear darker.

In order to make a full and detailed comparison of such observations with theory it is necessary to make accurate calculations of the dynamical scattering of electrons in the crystal, including the interactions of all beams of appreciable amplitude appearing in the diffraction pattern, Fig. 1(c), and then combining the diffracted beam amplitudes to calculate the image intensity, taking account of the effects of defocussing, spherical aberration and the limitations of objective aperture appropriate for the imaging conditions employed. Such calculations have previously been made by HEWAT[11,12] for images of Nb_2O_5 and other materials and are now being made for images such as that of Fig. 1 by Fejes (to be published).

In the present paper we take a less rigorous approach to the problem of image interpretation. We review first the simple phase object imaging theory and consider its limitations. We then consider modifications of this theory which appear to give a better qualitative account of the observations on lattice images which have been made to date.

II. Contrast from Thin Phase Objects

The effect on an incident electron beam, assumed to be coherent and of amplitude unity, of a thin specimen may be approximated by multiplication by a transmission function

$$q(xy) = \exp\{-i\sigma\varphi(xy) - \mu(xy)\}, \qquad (1)$$

where $\sigma = \pi/\lambda E$, E is the accelarating voltage of the beam, $\varphi(xy)$ is the projection of the potential distribution of the object in the beam direction and $\mu(xy)$ is the projection of an "absorption function" representing the effect of all processes by which some electrons are prevented from contributing to the image contrast, including the effect of a finite objective aperture size[13].

The modification of the relative phases of the diffracted beams by defocussing and by the spherical aberration may be represented by multiplying the amplitude in the back-focal plane of the objective lens, $Q(u,v)$, given by Fourier transform of (1), by the phase factor $\exp\{i\chi\}$ where

$$\chi = \pi\Delta\lambda u^2 - \tfrac{1}{2}\pi C_s\lambda^3 u^4. \qquad (2)$$

Here u is a radial coordinate ($u = r/f\lambda$, f is the focal length), Δ is the amount of defocus and C_s is the spherical aberration coefficient of the objective lens.

For thin biological samples, the approximation is usually made that $\sigma\varphi(xy) \ll 1$ and $\mu(xy) < \sigma\varphi(xy)$ so that (1) can be written

$$q(xy) \approx 1 - i\sigma\varphi(xy) - \mu(xy). \qquad (3)$$

The average value of $\varphi(xy)$ involved is that corresponding to the mean inner potential φ_0 since individual atoms are not resolved. For $\varphi_0 = 10$ eV and 50 eV electrons, the approximation (3) should be valid for thicknesses less than about 100 Å[13]. For crystals containing moderately heavy atoms, superimposed in projection, the maximum values of $\sigma\varphi$ will approach unity for a thickness of the order of 10 Å for 100 kV electrons and so the application of the approximation (3) should be severely limited.

The amplitude distribution in the image plane, obtained by Fourier transform of the amplitude distribution in the back-focal plane, will then be given by

$$\psi(xy) = q(xy) * \mathcal{F}[\exp(i\chi)] \qquad (4)$$

where the $*$ sign represents a convolution and $\mathcal{F}$ indicates Fourier transform operation. When the image intensity $\psi\psi^*$ is calculated with the approximation (3), only the real part of $\psi(xy)$ need be considered since the imaginary part contributes only second order terms in the quantities assumed small. Thus it may be assumed that the amplitude in the back focal plane is the real part of

$$Q(u,v)\exp\{i\chi\}$$

or

$$\Psi(uv) = \delta(u,v) - M(uv)\cos\chi + \sigma\Phi(uv)\sin\chi, \qquad (5)$$

where $M(uv)$ and $\Phi(u,v)$ are the Fourier transforms of $\mu(xy)$ and $\varphi(xy)$ respectively and the δ-function represents the unscattered incident beam.

The object of defocussing is to obtain an image intensity distribution as close as possible to that of an amplitude object, namely

$$I(xy) = 1 + 2\sigma\varphi(xy). \qquad (6)$$

From (5) it is seen that this will occur if the value of $\sin\chi$ is made close to ± 1 for as much of the range of the coordinate u as possible. For the "optimum defocus condition" of SCHERZER[5], the variation of $\sin\chi$ with u is as shown in Figure 2. For the low values of u, for which there is a large deviation from unity, a compensating contribution may be expected from $M(uv)\cos\chi$, since it is reasonable to expect $\mu(x, y)$ to have much the same form as $\varphi(xy)$.

Hence as a first rough approximation it may be assumed that the optimum defocus image may be similar to the amplitude object (6) and therefore subject to a simple intuitive interpretation. Inserting the value of the spherical aberration constant appropriate for our microscope, the JEM-100B, we find that this condition should occur for about 900 Å under focus[4].

3. Observations on $Ti_2Nb_{10}O_{29}$

The thickness of crystals giving images such as Fig. 1(a) is difficult to estimate with any precision. Approximate estimates have been obtained for particular crystals by making observations of the apparent width of planar faults as a function of crystal tilt and also by noting the change of contrast of the images for small tilts (see Section 5, below). The indication is that images which can be readily interpreted in terms of the crystal structure as in Fig. 1(a) and (b) are given for thicknesses up to 100 or 150 Å. For thicknesses beyond this the image is modified and soon becomes unrecognizable although in some cases the same image as for thin crystals reappears in a higher range of thicknesses of perhaps 700 to 1100 Å.

For crystals of 100 Å thickness the value of $\sigma\varphi$ corresponding to the mean inner potential φ_0 would be about 1. For the maxima of projected potential at the positions of heavy atoms the value could reach 10 or more. Hence the assumption of the simple theory that $\sigma\varphi \ll 1$ is clearly not valid.

In order to extend the validity of the theory to include somewhat larger values of $\sigma\varphi$, it is possible to include second order terms in the expansion of Equation (3). It has been shown by ERICKSON[14] that the additional terms introduced in this way in the intensity expression include an additional absorption effect. However these additional terms are complicated and difficult to appreciate intuitively. Also, as is well known for the case of the equivalent series of Born approximations for scattering theory, the expansion of the exponential of Eq. (1) in a power series gives terms which become rapidly more complicated and converge very slowly in the region for which the first-order approximation fails significantly. Hence the calculation of second order terms may be of use for thin biological objects in order to show the limitations of the first-order treatment but has little relevance for our purposes.

For thin biological objects the major contribution to the effective absorption function $\mu(x, y)$ comes from the elimination of scattered beams by the objective aperture. Since the resolution involved is of the order of 10 Å or more, the aperture is made small and a major part of the elastically scattered electrons is intercepted. For the crystal lattice images however, it is seen from Fig. 1(c) that a larger aperture is used to give the optimum resolution and contrast as suggested in Figure 2. Then

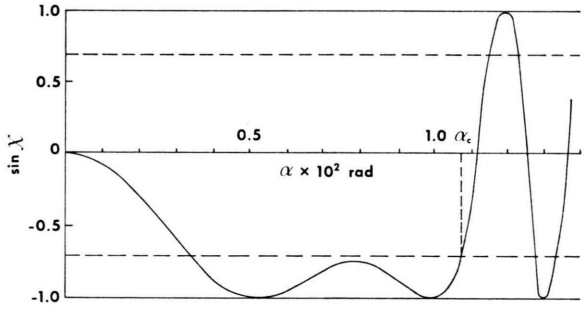

Fig. 2. The variation of $\sin\chi$ with the scattering angle $\alpha(\alpha = \lambda u)$ for the optimum defocus condition for thin phase objects. The desirable cut-off angle α_c corresponds to the objective aperture size indicated in Figure 1(c).

this contribution to the effective absorption function and so to the corresponding part of the expression (5) will be smaller. This may be compensated to some extent by a larger contribution to the absorption from thermal diffuse and single-electron scattering due to the presence of heavier atoms.

In spite of these severe limitations on the apparent validity of the simple thin phase-object contrast theory for our specimens, the predictions of this

theory seem to give a good account of at least the main features of the observations.

The image, Fig. 1 (a), which appears to be a good amplitude-object image of the projection of the crystal lattice was obtained with an underfocus of approximately 900 Å, as predicted[4]. The through-focus series, Fig. 3, shows that the in-focus image and images taken with an underfocus differing by more than a few hundred Å from this optimum value show very different intensity distributions. Preliminary calculations by P. Fejes suggest that the in-focus contrast is accounted for very well by the contribution of the spherical aberration term in (2) only.

It may be noted that, because there are major periodicities in the crystal of approximately 3 and 10 Å, it is to be expected that the out-of-focus images will show a tendency to repeat at intervals, d^2/λ, equal to about 2500 Å, in accordance with the theory of Fourier image formation[15]. Hence the first and last images of Fig. 3 tend to be similar.

More detailed observations of the images suggest, however, that the simple theory fails to account for the variations of contrast with crystal thickness and tilt. The theory would suggest that the peak value of $\varphi(xy)$ and therefore the image contrast would vary linearly with thickness and decrease with tilt away from a principle axis direction. This is not observed. The average intensity of the image decreases with thickness, presumably due to a uniform absorption, but the image contrast remains almost constant. With a tilt of the incident beam away from a principle direction the intensity distribution changes but the image contrast is not greatly affected. Here and in what follows we use the term "contrast" to imply a semi-quantitative measure of the range of relative intensity values present, irrespective of the form of the intensity distribution.

4. Simple Theory for Large Phase Changes

While a full account of the image intensities to be expected from crystals of finite thickness can be given best by extensive n-beam dynamical calculations, we have sought a reasonable basis for an intuitive type of interpretation which is more appropriate than the thin phase-object approximation described above.

In general, the effect on an incident electron wave of a crystalline or non-crystalline object can be considered as composed of phase changes, resulting from the transmission through the potential distribution, and Fresnel diffraction effects[16]. Fresnel diffraction effects may be neglected if the resulting spread of the wave (as judged by the width of the first Fresnel fringe) is less than the resolution limit of the electron microscope. For $\lambda \approx 0.04$ Å this suggests a thickness limit of about 100 Å for 2 Å resolution or 200 Å for 3 Å resolution. For smaller thicknesses than these we may make the phase-object approximation (1) but for our crystals we can not make the first-order approximation (3).

If we neglect absorption effects and the contribution of spherical aberration to the phase factor, χ, the Eq. (4) for the image amplitude obtained with a defocus distance Δ is given in one-dimensional form as

$$\psi(x) = \exp\{-i\sigma\varphi(x)\} * (i/\Delta\lambda)^{1/2} \exp\{-\pi i x^2/\Delta\lambda\}. \tag{7}$$

A convenient analytical form for this convolution may be obtained if we assume a special form for $\sigma\varphi(x)$, namely

$$\sigma\varphi(x) \equiv t(x) = \begin{cases} T & \text{if } |x| \leqq b/2 \\ 0 & \text{if } |x| > b/2, \end{cases}$$

for which we have the property $t^n(x) = T^{n-1} \cdot t(x)$. Then

$$\begin{aligned} \psi(x) &= \left[1 + \frac{t(x)}{T}(\exp\{-iT\} - 1)\right] * [(i/\Delta\lambda)^{1/2} \\ &\quad \cdot \exp\{-\pi i x^2/\Delta\lambda\}] \\ &= 1 + (i/4\pi)^{1/2}[(\cos T - 1) - i \sin T] \qquad (8) \\ &\quad \cdot \left[C\left\{\left(\frac{2}{\Delta\lambda}\right)^{1/2}\left(x + \frac{b}{2}\right)\right\} - C\left\{\left(\frac{2}{\Delta\lambda}\right)^{1/2}\left(x - \frac{b}{2}\right)\right\}\right. \\ &\quad - iS\left\{\left(\frac{2}{\Delta\lambda}\right)^{1/2}\left(x + \frac{b}{2}\right)\right\} \\ &\quad \left. + iS\left\{\left(\frac{2}{\Delta\lambda}\right)^{1/2}\left(x - \frac{b}{2}\right)\right\}\right], \end{aligned}$$

where $C(x)$ and $S(x)$ are the Fresnel cosine and sine integrals.

In the limiting case of very small width b, of the $t(x)$ function, so that $b/(\Delta\lambda)^{1/2}$ tends to zero, the differences between C and S functions in (8) give the differentials with respect to x, C' and S', so that

$$\begin{aligned} \psi(x) &= 1 + (i/\Delta\lambda)^{1/2} \\ &\quad \cdot b[\exp\{-iT\} - 1][C'(y) - iS'(y)], \end{aligned} \tag{9}$$

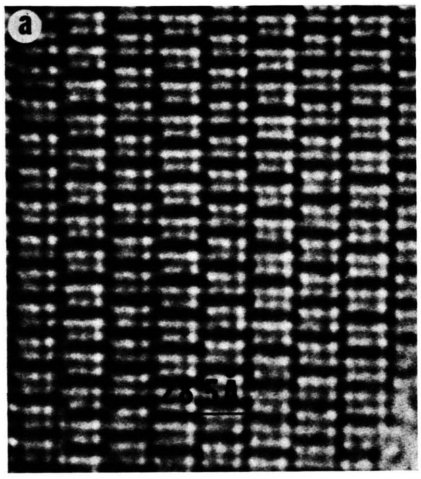

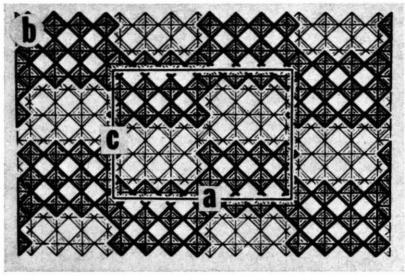

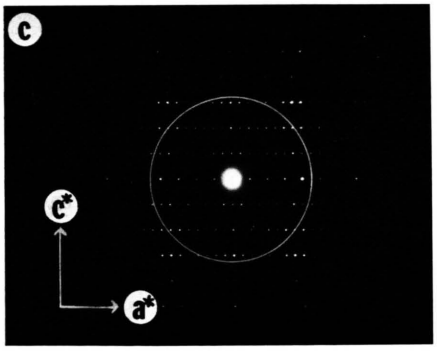

Fig. 1. (a) Electron micrograph of a thin portion of a crystal of $Ti_2Nb_{10}O_{29}$ taken with the incident beam parallel to the *b*-axis. (b) Diagram of the projection of the structure of $Ti_2Nb_{10}O_{29}$. Unit cell dimensions $a = 28.5$ Å, $c = 20.5$ Å. The structure is composed of two layers (dark and light lines) of metal atoms in oxygen octahedra (shaded squares). (c) Electron diffraction pattern of the crystal imaged in (a) with a circle drawn to indicate the objective aperture size.

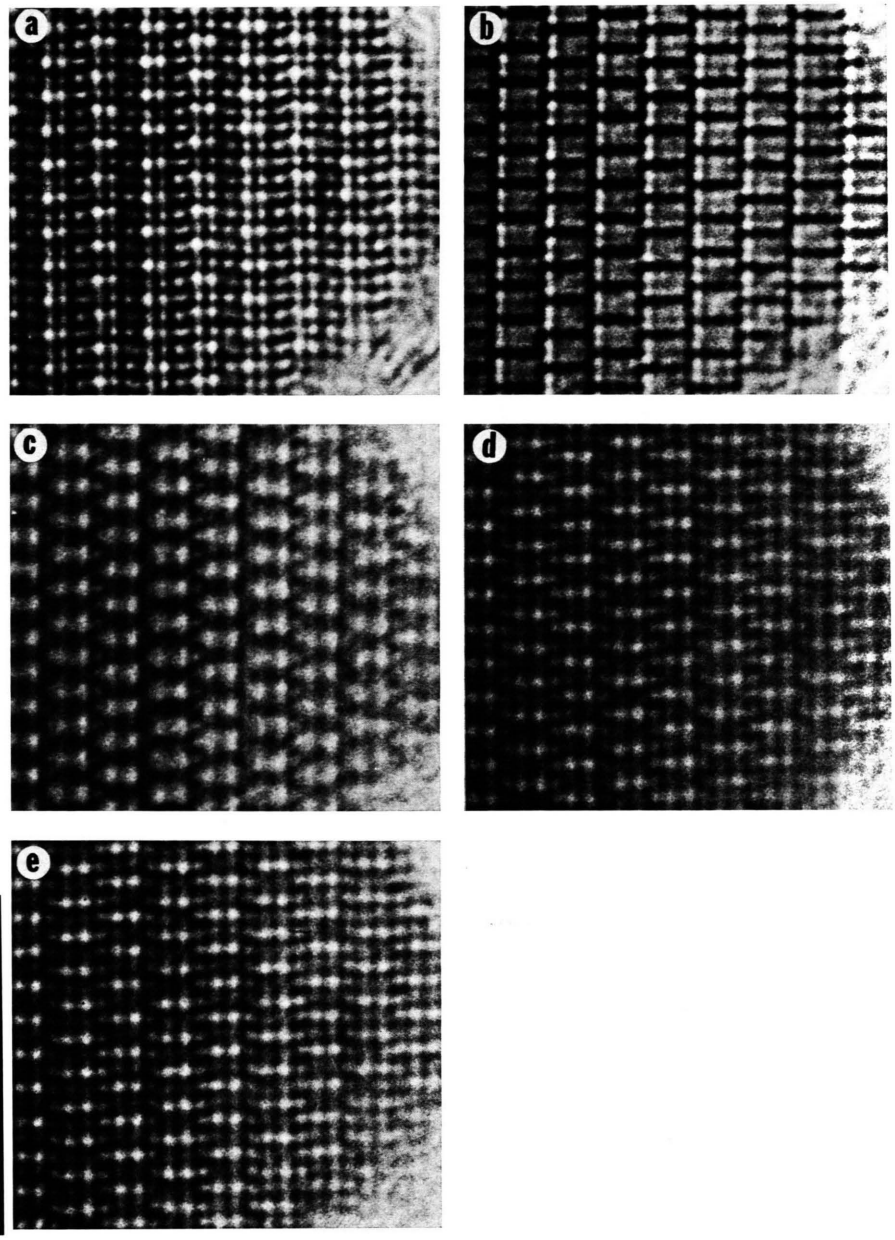

Fig. 3. Through-focus series of images of $Ti_2Nb_{10}O_{29}$ taken with values of the defocus distance Δ equal to (a) -1600 Å (b) -960 Å (c) -240 Å (d) 0 Å (e) $+240$ Å

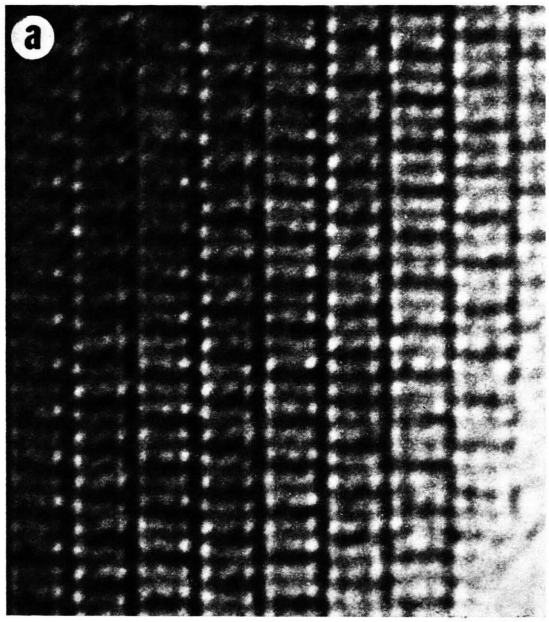

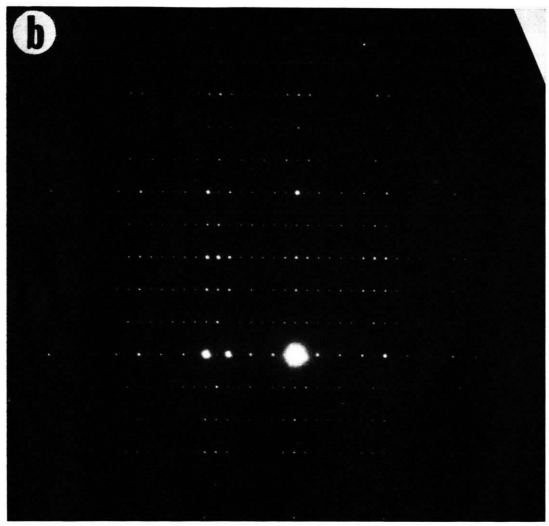

Fig. 6. (a) Electron micrograph of a crystal of $Ti_2Nb_{10}O_{29}$ tilted about the a-axis by 4×10^{-3} rad. away from the b-axis orientation. (b) Electron diffraction pattern corresponding to 6(a).

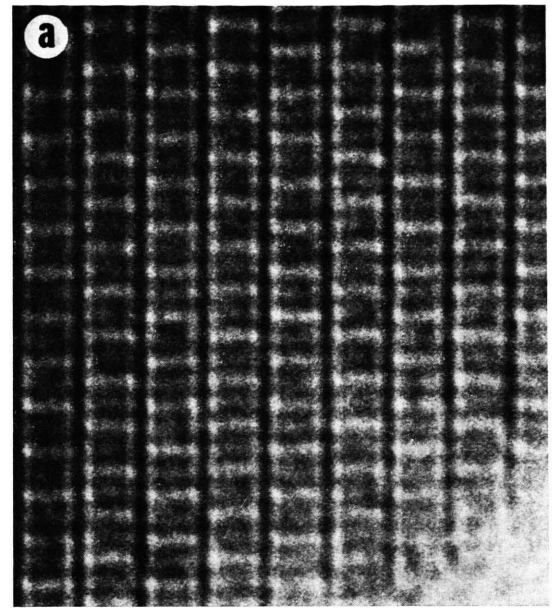

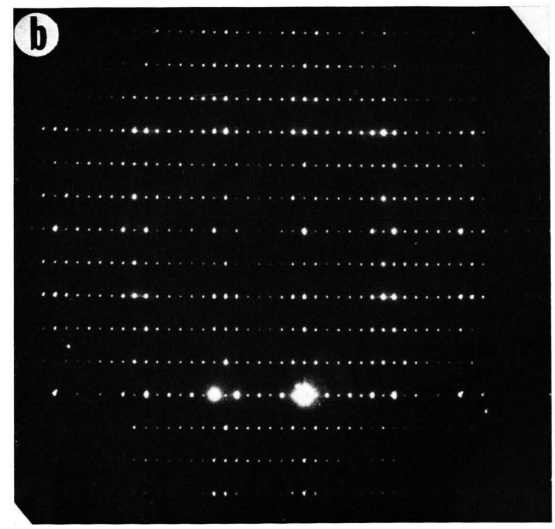

Fig. 7. (a) As for Figure 6(a) but tilted approximately 10^{-2} radians. (b) Electron diffraction pattern showing the tilt for 7(a).

where $y = (2/\Delta\lambda)^{1/2}x$, and the intensity distribution is then

$$I(x) = 1 + \left(\frac{b^2}{\Delta\lambda}\right)^{1/2}[\{C'(y) + S'(y)\}(\cos T - 1) + \{C'(y) - S'(y)\}\sin T] + \frac{b^2}{\Delta\lambda}[\{C'(y)\}^2 + \{S'(y)\}^2](1 - \cos T). \quad (10)$$

The functions $C' + S'$ and $C' - S'$ have central maxima of width near to $(\Delta\lambda)^{1/2}$ and then oscillate with periodicities decreasing with x. Hence if the intensity distribution for a defocus of a few hundred Å is viewed with a resolution of about 3 Å the image of a single $t(x)$ peak will show a central maximum surrounded by rapidly decreasing intensity oscillations.

For a projected peak of potential corresponding to a line of atoms, such that $\sigma\varphi(x)$ achieves values much greater than unity, we may consider $\sigma\varphi(x)$ to be made up of a large number of displaced $t(x)$ functions, as suggested in Figure 4. If the width

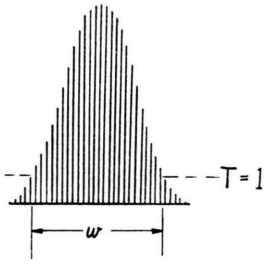

Fig. 4. Diagram suggesting the representation of a peak in the projected potential as made up of a large number of $t(x)$ functions.

of the $\sigma\varphi(x)$ peak is much less than that of the C' and S' functions or less than the resolution limit, the total amplitude may be made up of a large number of contributions of the form (9) and will be given to a first approximation by averaging (9) or (10) over T so that the cosine and sine terms drop out. The observed intensity distribution will be given approximately by

$$I(x) = 1 - w(\Delta\lambda)^{-1/2}\{C'(y) + S'(y)\} * R(x), \quad (11)$$

where w is the width of the peak in $\sigma\varphi(x)$, measured where the value of $\sigma\varphi(x)$ is approximately equal to unity. The spread function $R(x)$, of integrated value unity, is chosen so that convolution with $R(x)$ represents the loss of resolution due to the objective aperture size and the instabilities of the electron microscope. For example, one could assume

$$R(x) = (\pi d^2)^{-1/2}\exp\{-x^2/d^2\}, \quad (12)$$

where d is the minimum resolvable distance. The final, second-order term of (10) can be neglected if $w^2 \ll \Delta\lambda$ or $w \ll d$.

The form of the function $C'(y) + S'(y)$ is illustrated in Fig. 5 together with the form of the convolution with the function $R(x)$ given in (12) with $d = (\Delta\lambda/2)^{1/2}$.

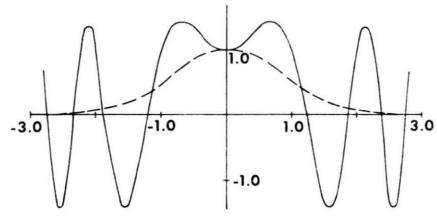

Fig. 5. The function $C'(y) + S'(y)$ (full curve) and the convolution of this function with a gaussian of half width unity (broken curve).

We have neglected in our treatment the effects of spherical aberration. In the thin phase-object theory of section 2 above, the inclusion of spherical aberration increases the optimum defocus value from about 400 to 900 Å. If we make the same assumption for the present case, it seems that the value of $(\Delta\lambda/2)^{1/2}$ to be considered is approximately 3 Å which is the same as the resolution of our images. Hence the broken curve of Fig. 5 should be revelant for our case.

From this simple result of Eq. (11) the interesting conclusion may be drawn that for a peak in the projected potential, $\sigma\varphi(x)$, of height much greater than unity, the contrast in the image will be almost independent of the height since it will depend only on the width of the peak if this is less than the limit of microscope resolution.

For example, a single peak in the projection corresponding to a single row of atoms will give approximately half the contrast of two parallel, unresolved rows of atoms. This is consistent with the appearance in Fig. 1(a) of the darkening corresponding to single and double rows of metal atoms [cf. Fig. 1(b)].

Also from (11) we deduce that when the incident beam is parallel to the crystal axis the contrast of the image will be almost independent of thickness, as observed.

In (11) the factor $(\Delta\lambda)^{-1/2}$ is compensated by an increase of the width of the $(C' + S')$ function by

the inverse factor. Hence when this function is convoluted with a spread function due to limited resolution, the intensity distribution and contrast should be approximately constant with defocus. Consideration of very small values of Δ is here excluded by the condition that $w^2/\Delta\lambda$ must be small. Also large values of Δ, for which interference effects between periodically repeated peaks give Fourier image phenomena[15], must also be excluded. In practice the images of the $Ti_2Nb_{10}O_{29}$ crystals showed a reasonable approximation to the optimum intensity distribution over a range of defocus values, Δ, from about 300 Å to 1200 Å.

5. Tilting Effects

The image of Fig. 1(a) was obtained with the incident electron beam very nearly parallel to the b-axis of the unit cell. The deviation from this principle orientation can be judged from the near-symmetry of the diffraction pattern, Fig. 1(b), to be no more than 10^{-3} rad. For a crystal 100 Å thick, a tilt of 10^{-2} rad. should broaden a projected peak of $\sigma\varphi(xy)$, due to a line of atoms, by 1 Å in the direction of tilt and this may be expected to have a visible effect on this image. The micrograph, Fig. 6(a) was obtained with a tilt about the a-axis of 4×10^{-3} rad. as judged by the diffraction pattern, Figure 6(b). The effect of the broadening of the features resulting in a poorer resolution of the fine structure in the tilt direction is clearly visible. For the larger tilt of 10^{-2} radians, as suggested by the diffraction pattern, Fig. 7(b), the image, Fig. 7(a) has been modified strongly. Hence the sensitivity of the image to a tilt of the crystal is roughly as suggested by simple geometric considerations.

For the thin phase-object approximation the contrast of a single sharp peak in $\sigma\varphi(xy)$ of width less than the resolution limit will depend only on the integrated weight of the peak. Hence for a peak due to a single line of atoms, extended into a line in projection as the crystal is tilted, the contrast will remain constant while the line is shorter than the resolution limit, but will decrease as greater tilts extend the length of the line beyond the resolution limit. On the other hand, the conclusion to be drawn from (11) is that for thick phase-objects, the contrast of the projected peak will at first increase with tilt as the width w increases up to the resolution limit. Then for larger tilts, since the length of the peak within the region of a spread function remains constant, the contrast will remain unchanged, although the detailed form of the intensity distribution will vary.

While it is not easy to make detailed comparisons of contrast in practice or to predict contrast behaviour for complicated crystal structures, our observations to date seem to be more nearly in agreement with what might be expected for a thick phase-object using these arguments.

The change in the nature of the contrast along lines parallel to the c-axis in Fig. 7(a) as compared with 1(a) can be understood by reference to Figure 8. Along a line of metal atom positions parallel to the c-axis the projection of the potential will be a series of sharp peaks represented by dots in Fig. 8(a)

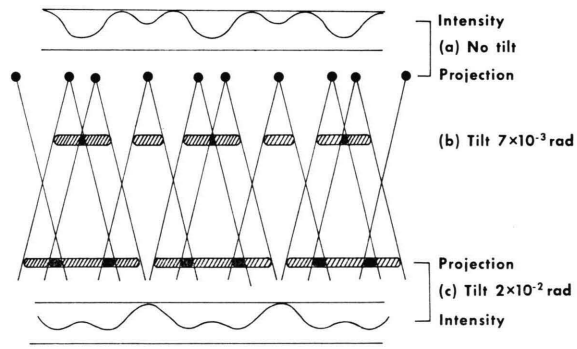

Fig. 8. Diagram illustrating the change of contrast with tilt along lines parallel to the c-axis of the $Ti_2Nb_{10}O_{29}$ structure for a crystal approximately 150 Å thick. (a) The projection and image intensity for no tilt. (c) The modification of the projection and image intensity for a tilt of approximately 10^{-2} radians, showing the apparent reversal of contrast.

for the untilted crystal with a resulting intensity variation as shown, when the closer pairs of dots are not resolved. With increasing tilt the dots spread out into rods which overlap more and more as in 8(b) and 8(c). For 8(c) the minimum value of $\sigma\varphi(xy)$ may be subtracted out since it represents a uniform phase change, leaving a distribution with only one broad minimum which may be expected to give the intensity distribution sketched, with one broad white band per 10 Å repeat distance rather than the two sharper white bands of 8(a). Thus the main features of Fig. 7(a) are reproduced.

Tilting experiments such as these confirm the conclusion to be drawn from Eq. (11) that the intensity at a point in the image for such crystals

is not linearly related to the value of the projected potential distribution at that point. Hence it is clear that images obtained with different tilts can not be simply combined to give stereo images of the structure in three dimensions.

In general it would seem that while the intensity distributions may be predicted rather simply for known or postulated structures, when the electron beam is almost parallel to a principal axis, there may well be ambiguities of interpretation which will complicate the process of deducing completely unknown structures directly from observed intensity distributions.

6. Crystal Periodicities and Symmetry

It was argued by COWLEY and MOODIE[17] and COWLEY et al.[18] that within certain limitations, the symmetry of the projection of the crystal lattice in the beam direction will be maintained in all dynamical diffraction processes. A more complete discussion of the limitation to this rule was given by GJØNNES and MOODIE[19].

Within the range of applicability of the phase-object approximation it is clear that all symmetry elements of the projection of the potential, $\varphi(xy)$, must be maintained in the image, irrespective of crystal thickness or of microscope focus or spherical aberration.

This rule does not exclude, of course, the well-known occurrence of apparent half-spacings or other submultiples of crystal lattice periodicities. It does exclude the occurrence of double spacings or of any greater periodicities than actually occur in the crystal lattice.

It is interesting to note in the images of $Ti_2Nb_{10}O_{29}$ that there is a definite 28 Å periodicity visible. Alternate dark lines (of 14 Å spacing) show different contrast variations whereas, from the structure deduced from X-ray diffraction, Fig. 1(b), it is clear that all these dark lines should show the same contrast as a result of planes of reflection parallel to the c-axis at $a/4$ and $3a/4$. Hence it must be concluded that the structure determined from X-ray diffraction is wrong in this respect.

In the X-ray study[10], no evidence was found of any ordering of the Ti and Nb atoms among the metal atom sites. It may be that these atoms are in fact ordered, giving the 28 Å periodicity observed. Then the range ot ordering could have been too small in the very much larger crystals used for the X-ray studies to allow the effects of ordering to be detected in the sharp Bragg reflections. On the other hand it may be that the image intensities as given approximately by Eq. (11) are much more sensitive to minor structural variations than X-ray diffraction intensities in the case of this particular compound. We have not as yet produced a model for a fully ordered structure which gives a satisfying explanation for the contrast observed in the electron microscope images.

Acknowledgement

This work was supported by the National Science Foundation Area Development Grant in Solid State Science (No. GU 3169).

[1] J. G. ALLPRESS, J. V. SANDERS, and A. D. WADSLEY, Acta Cryst. B **25**, 1156 [1969].
[2] J. G. ALLPRESS, J. Solid State Chem. **1**, 66 [1969].
[3] J. G. ALLPRESS, Materials Res. Bull. **3**, 707 [1969].
[4] N. UYEDA, T. KOBAYASHI, E. SUITO, Y. HARADA, and M. WATANABE, in Microscopie Electronique, 1970, Vol. **1**, 23 [1970].
[5] O. SCHERZER, J. Appl. Phys. **20**, 20 [1949].
[6] R. D. HEIDENREICH and R. W. HAMMING, Bell Syst. Tech. J. **44**, 207 [1965].
[7] Claire B. EISENHANDLER and B. M. SIEGEL, J. Appl. Phys. **37**, 1613 [1965].
[8] H. P. ERICKSON and A. KLUG, Ber. Bunsen Ges. Phys. Chem. **71**, 1129 [1970].
[9] Sumio IIJIMA, J. Appl. Phys. **42**, 5891 [1971].
[10] A. D. WADSLEY, Acta Cryst. **14**, 660 [1961].
[11] Elizabeth HEWAT (previously Chidzey) M. Sc. Thesis, University of Melbourne, 1970.
[12] J. G. ALLPRESS, Elizabeth HEWAT, A. F. MOODIE, and J. V. SANDERS, (In preparation).
[13] G. R. GRINTON and J. M. COWLEY, Optik **34**, 221 [1971].
[14] H. P. ERICKSON (In preparation).
[15] J. M. COWLEY and A. F. MOODIE, Proc. Phys. Soc. London B **70**, 486 [1957].
[16] J. M. COWLEY and A. F. MOODIE, Acta Cryst. **10**, 609 [1957].
[17] J. M. COWLEY and A. F. MOODIE, Acta Cryst. **12**, 360 [1959].
[18] J. M. COWLEY, A. F. MOODIE, Shizuo MIYAKE, Satio TAKAGI, and Fuminori FUJIMOTO, Acta Cryst. **14**, 87 [1961].
[19] J. K. GJØNNES and A. F. MOODIE, Acta Cryst. **19**, 65 [1965].